Applied Physics B
Lasers and Optics

CrossMark

Thermal lens in a liquid sample with focal length controllable by bulk temperature

Krzysztof Dobek[1] · Mikołaj Baranowski[1] · Jerzy Karolczak[1,2] · Dariusz Komar[1] ·
Kamila Kreczmer[1] · Jerzy Szuniewicz[3]

Abstract An experimental and numerical investigation of the applicability of the temperature-controlled focal length of a thermally induced lens is reported. The thermal lens is formed as a result of absorption of a heating laser beam. Numerical simulations and experimental results show that changing the bulk temperature of the material of the lensing element allows for the selection of its focal length. The range of focal length changes for an example lens is given.

1 Introduction

In response to the rising demands of new technologies, several different ways have been proposed to overcome the main disadvantage of a rigid lens: its fixed focal length, *f*. An artificial flexible intraocular lens has been developed [1], the shape of which is controlled by the human eye's muscles. A polymer variable focal length lens has been presented, in which a flexible polydimethylsiloxane membrane is used to form the lens surface which is deformed by e.g. fluidic pressure applied by an external syringe pump [2–5]. An electrode-based liquid lens, in which the liquid plays the role of electrolyte deformed by electric field formed between two insulated electrodes [6–8], has been tested as well.

✉ Krzysztof Dobek
dobas@amu.edu.pl

1   Department of Physics, Adam Mickiewicz University, Umultowska 85, 61-614 Poznan, Poland

2   Center for Ultrafast Laser Spectroscopy, Adam Mickiewicz University, Umultowska 85, 61-614 Poznan, Poland

3   Adam Mickiewicz High School, H. Cegielskiego 1, 61-862 Poznan, Poland

In this paper, we propose a new solution, which is an improvement to recent propositions given in [9–11]. In contrast to many of the above-cited ideas, which rely on modification of the lens shape, one can induce a refractive index distribution, ∇n, that acts as a lens, without changing the shape of the lensing element. Optical elements with such n distribution, called GRIN (*gradient refractive index*), are e.g. lenses or fibres, but these elements have ∇n fixed. Therefore, they do not conform to the idea of flexible optical elements (as used e.g. in adaptive optics). Meanwhile, such ∇n can be induced thermally, by irradiation of the thermal lensing element by a heating laser beam, absorbed by this elements material, or by controlled electrical heating of the thermal lensing element [12]. As shown by the authors of Refs. [9–11], ∇n formation can lead to the formation of a few millimetre (thus macroscopic)-size aperture thermal lenses whose focal length depends on the heating laser intensity. However, the authors of these two works did not take into account that ∇n at a selected heating laser intensity can depend as well on the bulk temperature of the thermal lens element, irrespective of this element being a liquid [9, 10] or solid [11]. This particular dependence was the subject of our interest, and this work presents the results of our studies.

In principle, the laser can also induce the nonlinear Kerr effect or electrostriction force—both of which can lead to nonzero ∇n [13]. In this work, we assume these effects negligible and we focus only on the thermo-optical effect. It follows from nonzero thermo-optical $\partial n / \partial T$ parameter of the medium illuminated by heating laser. We present results for a liquid thermal lens material, but thermal lenses can be formed in solids as well, e.g. in glasses. This last case is more attractive from the application point of view. Solids are free from convection and easier to use in different optical set-ups. Additionally, due to the thermal expansion,
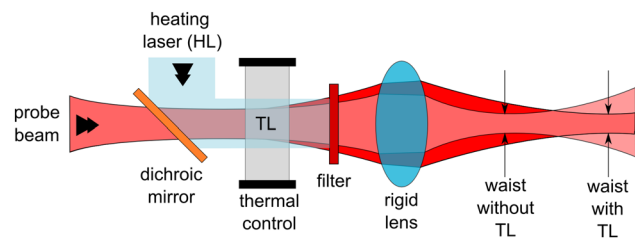
Fig. 1 An example application of a thermal lens (TL). The heating laser beam (HL) forms a thermal lens in the TL element whose temperature is controlled. Next, the filter stops the HL and let the probe beam pass. Depending on the presence and focal length of the TL, the probe beam waist is found at different positions after focusing by the rigid lens. In most situations, the HL is of wider diameter than the probe beam. In some, as described in Sect. 3.1 it is narrower

and the thermally dependent photoelastic effect the thermal lens formed in solids may be convergent [14], while in liquids a thermal lens is always divergent due to the negative thermo-optical coefficient of liquids [15]. On the other hand, liquids are a natural environment for different types of photophysical processes or photochemical reactions. These processes may lead to very strong dependencies of ∇n on bulk temperature. Because our team has studied such temperature-dependent photophysical/photochemical processes for a considerable time now, we decided to use a liquid thermal lens. However, we did so being fully aware of the complexity of using liquids instead of solids in optical set-ups. Therefore, this work should be treated as a proof-of-principle study showing new possibilities in thermal lens focal length control, in carefully selected solids as well.

The device containing a thermal lens can work in a way presented in Fig. 1.

In most cases, the heating laser beam is broader than the probe beam, as the latter has to pass through the region of the thermal lens element in which ∇n was generated. As shown in Fig. 1, the thermal lens is divergent, which is a reflection of the negative $\partial n / \partial T$ thermo-optical factor that characterizes liquids. The filter stops the heating laser beam. It is assumed no thermal lens is formed inside this filter so the filter has to be a dichroic mirror, a polarizing beam splitter or the heating laser beam power is insignificantly low after the thermal lensing element so an absorbing filter may be used. The rigid lens is only present to show how such a system may act as a flexible focal length converging device. Black bars on the top and bottom of the thermal lens element represent the bulk temperature (T_b) control device. According to [16, 17], for continuous heating laser illumination, the focal length of the thermal lens as shown in Fig. 1 is given as:

$$f = \frac{\pi \omega_e^2 k}{2.3 A P (1 - \varphi_F \lambda_e / \langle \lambda \rangle) \frac{\partial n}{\partial T}}, \tag{1}$$

where A and k are the absorbance at excitation wavelength λ_e and the thermal conductivity of the thermal lens material, P and ω_e are heating laser power and waist (localized in thermal lens centre) and φ_F and $\langle \lambda \rangle$ are the thermal lens material fluorescence quantum yield and fluorescence spectrum first spectral moment. The term in parentheses in Eq. (1) describes the efficiency of light-to-heat conversion in absorbing thermal lens material [18]. From the above parameters, all except P and λ_e can depend on temperature. Assuming a normal incidence of the heating laser beam at the thermal lens element surface and a long Rayleigh distance of the heating laser beam compared with the element length, one can assume that ω_e is T independent. In most cases, it can also be assumed that $\partial^2 n / \partial T^2 = 0$. However, if the thermal lens material is a solution of a dye in a liquid $A(\lambda_e)$, φ_F and $\langle \lambda \rangle$ are likely to be T dependent, as we have shown for two coumarin dyes recently [19]. For most liquids, k is temperature dependent as well [20]. Therefore, f can be controlled by changing the bulk temperature of the thermal lens element.

2 Simulations

In order to check whether f may depend on T_b, we performed numerical simulations of the thermal lens in COMSOL Multiphysics software by means of the finite element methods. We used the heat transfer in fluids module to simulate the thermal lens formation. The thermal lens element was modelled as of rectangular shape $20 \times 20 \times 5$ mm in size, and we assumed it to be a solution of coumarin 153 in ethanol. Initially, all dependencies for this particular dye solution: $A(T_b)$, $\langle \lambda \rangle(T_b)$ and $\varphi_F(T_b)$ were taken from our earlier work [21]. But, as we found that the experimental $\varphi_F (T_b)$ dependence for coumarin 153 in ethanol compensates the effects of $A(T_b)$ and $\langle \lambda \rangle(T_b)$ on f, we arbitrarily assumed $\varphi_F(T_b) = 0.05 + (T_b - 283.15)*0.0075$, a dependence we expected from the experimental material we used. Thus, our simulated thermal lens material did not correspond to any particular material from the ones already thermally investigated, but was similar in properties to them. The initial temperature of the simulated thermal lens element was set to T_b. A heat transfer was assumed to take place through all faces of the element at a rate of 10 W/(m²K). The temperature of the surrounding of the thermal lens element was also set to T_b. The simulation was performed in a time-resolved regime.

The final results are reported for 1500 s after simulation start. The heating laser was assumed to have $P_{HL} = 40$ mW of power, 405 nm wavelength and 5 mm waist diameter localized at the front of the thermal lens element. As it is known that the heating laser beam intensity profile strongly affects thermal lens properties [22], we performed

simulations for a Gaussian and top-hat intensity profile of the heating laser beam. As reported in the literature, the top-hat profile has been found to edge the Gaussian one, in terms of spherical aberrations of the thermal lens element. Figure 2 presents the simulated profiles of T and n in the y and x directions perpendicular to the heating laser optical axis (z). They were obtained for the heating laser beam with a top-hat intensity profile. These results were obtained at $T_b = 283$ K at the centre of the thermal lens element. Figure 3 presents the temperature effect on the focal length of the thermal lens element determined through ray tracing in COMSOL. We used photonic ray tracing method as proposed by Urzhumov [23]. The application of this procedure was tested by successfully simulating a GRIN fibre and comparing its operation with the analytical solution [24]. Probe rays entered the thermal lens through its front face (xy plane) symmetrically on both sides of the heating laser
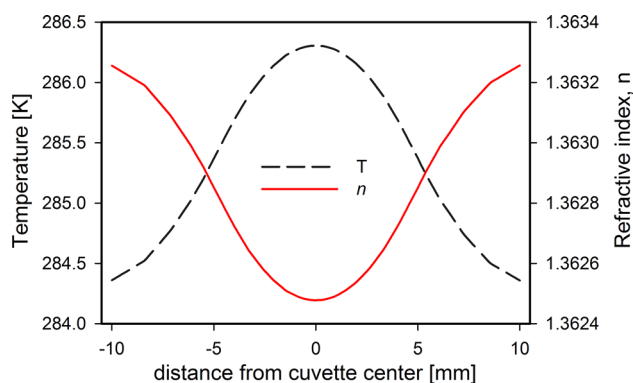
beam optical axis, with a 2-mm step. Thus, the values given in Fig. 3 legend are the distances of the rays from the centre of the heating laser at the thermal lens element entrance. Focal lengths were determined as the distance between the element back face and the point at which two rays exiting the element crossed. These were rays that entered the thermal lens front face at the same distance from the heating laser beam axis. Obviously, due to the diverging character of the simulated thermal lens, the crossing point was located in front of the element.

For heating laser beam with top-hat profile, small aberrations are observed for the rays entering the thermal lens in the heated region. A dependence on T_b is also observed, as absolute f increases with temperature. For heating laser Gaussian profile, clear spherical aberrations were observed. Nevertheless, an $f(T)$ dependence was obtained.

3 Experiments

3.1 Thermal lens spectroscopy

Experimental verification of the feasibility of thermal lens f control through T_b change started by building a spectroscopic thermal lensing set-up (Fig. 4). We followed the solution given by Shen et al. [18]. The heating laser was a $\lambda_e = 405$ nm, $P = 40$ mW diode laser. The probe laser was a $\lambda_p = 633$ nm, 12 mW He–Ne laser. A computer-controlled shutter was used to open the heating laser for a period of 200 ms, during which the sample was heated. The heating laser beam was focused to a waist $\omega_e = 150$ µm at the centre of an $L = 4$ mm optical path fluorescence cuvette. The cuvette was placed in a recirculating holder attached to a chiller/heater. The holder was heating the TL element from bottom and two opposite sides parallel to the optical axis of the set-up. The probe beam had diameter $\omega_{1p} = 700$ µm at the cuvette, and its waist was located at $Z_1 = 145$ mm

Fig. 2 Temperature (T, in y direction) and refractive index (n, in x direction) distributions in the simulated thermal lens at 283 K, z-propagation direction of the heating laser beam
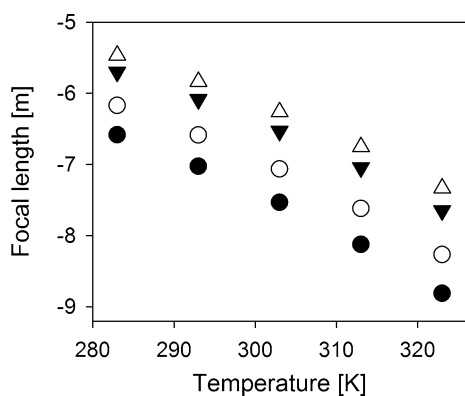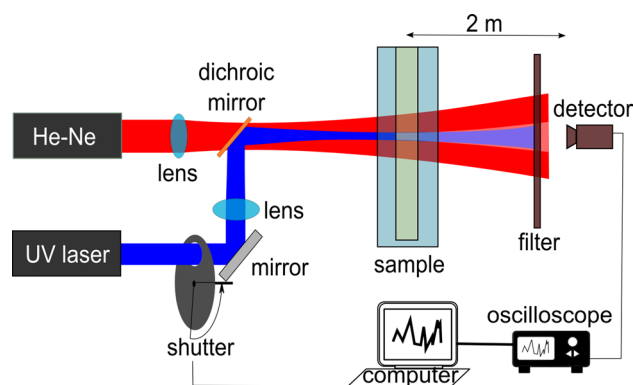

Fig. 3 Focal lengths obtained from thermal lens simulations in COMSOL, obtained from rays entering the thermal lens element orthogonally at different distances from its optical axis (*open triangles*—1 mm, *filled triangles*—3 mm, *open circles*—5 mm, *filled circles*—7 mm)

Fig. 4 Experimental set-up designed for thermal lensing spectroscopy

from the cuvette centre. The probe signal was collected at the probe beam centre, 2 m away from the cuvette, using a photodiode preceded by a filter and small diaphragm and connected to a digital USB scope. The scope was triggered by the same signal that was opening the shutter. All beam diameters were determined using a high-sensitivity USB camera and home-made beam profiling software, based on the ISO-11146-1 standard method [25].

According to Ref. [18], the signal recorded by the photodiode can be described by:

$$I(t) = \left[1 - \frac{\theta}{2} \arctan\left(2mV\left(((1+2m)^2 + V^2)(t/t_c) + 1 + 2m + V^2 \right)^{-1} \right) \right]^2,$$
(2)

where $m = (\omega_{1p}/\omega_e)^2$, $V = Z_1/Z_c$ and $Z_c = \pi\omega_{0p}^2/\lambda_p$ is the confocal distance of the probe beam of waist ω_{0p}. The parameter θ is connected to f (Eq. 1) through $f = -(\pi\omega_e^2)/(\lambda_p\theta)$, and t_c is the thermal relaxation time that characterizes the thermal lens medium. In order to determine $f(T_b)$, one can measure $I(t)$ at several temperatures, and after fitting the signal with Eq. 2, θ and t_c can be obtained. We followed this procedure for several different solutions of coumarins 151, 153, 102 and for 4-aminophthalimide (4-AP) dissolved in different protic solvents. Additionally, we did the same for 4-AP dissolved in a mixture of dimethyl sulphoxide (DMSO) and water at volume ratios of 70 %:30 %, 85 %:15 % and 90 %:10 % in favour of DMSO (at room T).

From our studies and others, it is known that 4-AP forms very strong hydrogen bonds with water that promote its non-radiative deactivation from the excited state, so that φ_F (4-AP) = 0.83 in DMSO while 0.02 in water. Water also increases the red shift of $\langle\lambda\rangle$ versus λ_e [26]. Selection of a mixture of DMSO and water was dictated by observations of strong effect of temperature on the energy of hydrogen bonds that 4-AP forms with e.g. water molecules in such mixtures [27, 28]. Thus, we expected that temperature may most significantly affect f in such a solution of 4-AP, and indeed, it was confirmed for all thermal lens media we selected. Figure 5 shows $f(T_b)$ for a 10^{-3}M 4-AP solution in the most hydrated DMSO + water mixture. The focal length decreases with increasing temperature, which means the thermal lens become less divergent. No thermal lensing was observed for pure DMSO + water mixture with no 4-AP added. Thus, these preliminary results indicated that temperature may be used as f controlling factor, in accordance with the results of the simulations.

3.2 Macroscopic aperture thermal lens

In order to check whether the flexible thermal lens can be used as an imaging element with "large" aperture, a new set-up was built, as shown in Fig. 6. This time the heating laser beam was of wider diameter than the probe beam. Using a spatial filter, the heating laser beam was transformed into a Gaussian one. The probe beam was collimated. At the cuvette with 4-AP in DMSO + water, both beams had waists $\omega_e = 1.34$ mm and $\omega_{0p} = 0.43$ mm. The He–Ne probe beam was attenuated to $P = 150\ \mu$W in front of the sample, as it has been found that at the geometry used, this beam was forming a thermal lens in the sample, without a heating laser beam present. This self-focusing effect led to unwanted slow oscillations of the probe beam width behind the sample, with a period in the order of minutes and of very small but resolvable amplitude. Because of this attenuation, behind the sample the probe beam was focused by a lens and finally its width was measured using a camera placed on a linear stage and beam profiling software. To separate the heating laser beam from the probe, a prism was placed in their path. Note that in the thermal lens spectroscopic set-up (Fig. 4) thermal lensing induced by He–Ne beam was not recorded as in this case the probe beam was much wider than the heating laser beam, and we were measuring signal changes in the order of milliseconds not minutes. In the "macroscopic" measurement, determination of the probe beam waist radius and location by the beam profiler camera took a few minutes and had to be done with and without the heating laser beam. Therefore,
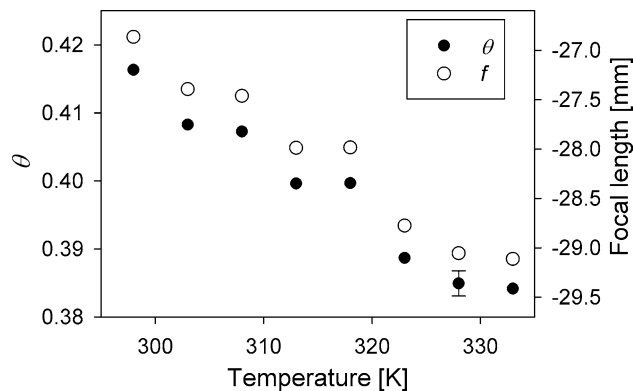

Fig. 5 Temperature effect on θ and f for 4-AP in DMSO + water mixture measured using the spectroscopic thermal lensing system
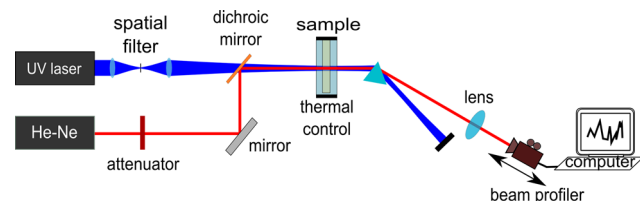

Fig. 6 Experimental set-up used to determine temperature dependence of a "macroscopic" thermal lens, formed in the 4-AP in DMSO + water mixture

any long-time fluctuations of the probe beam waist had to be eliminated. The cuvette with the sample was aligned horizontally, and both laser beams were passing the sample vertically so that all the effects related to convection had radial symmetry.

Next, assuming the Gaussian character of the beam, the thermal lens element focal length was determined, using the standard Gaussian beam propagation rules [24]. To do this, we measured the distances of the probe beam waist from the lens focusing this beam on the camera, this lens focal length and distance from this lens to the sample. For the sake of simplicity, we omitted the prism in the calculation, as its presence was not modifying our final conclusions.

Figure 7 presents the temperature dependencies of the thermal lens focal length measured in the xz and yz planes, where z is the probe and heating laser beams propagation direction. The uncertainties shown in Fig. 7 were determined using propagation of the uncertainties of the probe beam waist radius and location determined using beam profiling.

As can be seen, the effect is similar to the one obtained in the spectroscopic set-up. The thermal lens absolute focal length value increases with temperature. The range of the focal lengths and its changes are similar to those obtained from simulations. A difference between the values obtained for the xz and yz planes is visible. Two sources of such difference were identified. The first is that the prism used to separate the probe from the heating laser was potentially affecting the probe beam waist in the plane of the experimental set-up, see scheme in Fig. 6. Such effect should be constant with time (and temperature). However, if the angle at which the probe beam was entering the prism was changing slowly with time, then the effect of the prism would change with time as well. And this change would be seen only in the direction parallel to the refractive plane of the
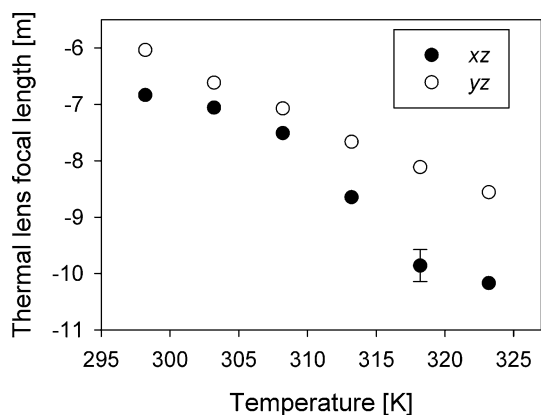
prism. Changes in mentioned angle could take place due to slow variation in probe beam propagation direction resulting from slow misalignment of our set-up.

It could follow as well from another effect. Due to the limited power of our heating laser, its beam was not significantly wider than the probe beam. Meanwhile, as shown by our simulations and known from the literature [22] a thermal lens has parabolic character only in the area close to the heating laser beam optical axis. As a consequence, with the experiment time, the misalignment of one of the beams could slowly increase and cause differences in the probe beam widths, which in consequence after the prism could lead to unwanted changes in probe beam waists measured by the beam profiler. In order to check whether a thermal lens can be seen in DMSO + water mixture only, without 4-AP, a probe beam width was monitored by the beam profiler both with and without heating laser at the same temperatures as used for 4-AP solution. No changes in probe beam profile were observed, which indicates that heating laser was absorbed neither by water nor by DMSO.

Taking into account T_b was set by heating the cuvette with the thermal lensing material only from three sides, one could attempt to connect the differences in f shown in Fig. 7 with some asymmetric temperature gradient present in the cuvette. Such gradients were, for example, observed in [12]. We did not find any significant dependence of the probe beam waist (position) on T_b when the heating laser beam was absent. Obviously, such dependence was found when the heating laser was present. Therefore, we concluded the bulk temperature in our set-up was set homogeneously enough to let assume no T_b gradient is present in the thermal lens. Note that obtaining such homogeneity was facilitated by the fact we waited 15 min for each T_b to stabilize.

Our results show that our set-up for the bulk temperature control of the thermal lens focal length allows a change in f in a range similar to that obtained for a thermal lens controlled by heating laser power. The authors of [10] obtained the values from approximately $f = -2.5$ to -0.5 m for the heating laser power range $P_{HL} = 2$ to 8 mW in a solution of the sunset yellow dye in ethanol. In [11], the values of f are reported to vary from 1.25 to 10 m for P_{HL} changed from 0.5 to 6 W for a thermal lens formed in a colour glass filter. Our results show that temperature stabilization of the thermal lens material is a requirement for a heating laser power-controlled thermal lens. But, additionally it can be used as a focal length controlling tool. The disadvantage of such a method is obviously the relatively slow bulk temperature setting time. On the other hand, it does not require modulation of the heating laser power and thus allows a stable long-time heating laser activity which extends the laser lifetime. The heating laser power can also be relatively low.

The thermal lens element proposed in this work can also react passively to changes in temperature. For instance, one

Fig. 7 Temperature effect on the thermal lens element focal length for 4-AP in DMSO + water mixture measured using the "macroscopic" thermal lensing system. *Closed circles* correspond to f measured in the xz plane and *open circles* to the values obtained in the yz plane, z-propagation direction of the probe and heating laser beams

can imagine such a set-up put in a laser resonator, in order to re/defocus the laser beam in response to temperature changes inside the laser cavity. Next, one may very well use another thermal lens material, whose efficiency to convert absorbed energy into heat is much more dependent on temperature than the one we used. There are many photochemical materials in which, for instance, the rates of light induced reactions are strongly dependent on temperature (e.g. [29]). These reactions in most cases deactivate the material through radiationless paths, that is, they lead to the heating of the sample. But, these materials have not been investigated fully, and it should be checked before use whether change in temperature of one effect controlling thermal lens focal length is not countervailed by another. Nonlinear absorption (saturation), which may appear in the heating laser power-controlled thermal lens, may be neglected in the temperature-controlled thermal lens as it is always possible to use a material whose absorption spectrum does not change with temperature, but e.g. fluorescence quantum yield does. Heat convection in liquids is a limitation, because it makes the thermal lens orientation dependent. Therefore, the thermal lens material should be a solid and polymer-based samples doped with chromophore containing molecules seem to be the best choice, especially thermochromic polymer-based materials [30].

4 Conclusions

We have shown that it is possible to modify the focal length of a thermal lens by changing its bulk temperature. This procedure could be used e.g. in a laser resonator in order to react to unwanted laser beam focusing/defocusing. While temperature control is relatively slow, the method proposed may be of interest to those looking for a flexible lens passively changing its focal length as a result of bulk temperature change.

References

1. NuLens® intraocular lens, NuLens Ltd. Herzliya, Israel, US patent 20070244561 A1
2. J. Chen, W. Wang, J. Fang, K. Varahramyan, J. Micromech. Microeng. **14**, 675–680 (2004)
3. M. Agarwal, R.A. Gunasekaran, P. Coane, K. Varahramyan, J. Micromech. Microeng. **14**, 1665–1673 (2004)
4. D.-Y. Zhang, V. Lien, Y. Berdichevsky, J. Choi, Y.-H. Lo, Appl. Phys. Lett. **82**, 3171–3172 (2003)
5. M. Blum, M. Büeler, C. Grätzel, M. Aschwanden, in *Proceedings of SPIE 8167, Optical Design and Engineering IV*, 81670 W (2011)
6. S. Kwon, L.P. Lee, in *Proceedings of 11th International Conference on Solid State Sensor and Actuators Transducers* **1342**, 1348–1351 (2001)
7. B. Berge, in *Proceedings of 18th IEEE International Conference on Micro-Electro-Mechanical Systems* 227–230 (2005)
8. C.C. Cheng, C.A. Chang, J.A. Yeh, Opt. Express **14**, 4101–4106 (2006)
9. H.D. Doan, Y. Akamine, K. Fushinobu, Int. J. Heat Mass Transf. **55**, 2807–2812 (2012)
10. H.D. Doan, Y. Akamine, K. Fushinobu, Int. J. Heat Mass Transf. **55**, 7104–7108 (2012)
11. V. Quetschke, J. Gleason, M. Rakhmanov, J. Lee, L. Zhang, K. Yoshiki Franzen, C. Leidel, G. Mueller, R. Amin, D.B. Tanner, D.H. Reitze, Opt. Lett. **31**, 217–219 (2006)
12. Z. Liu, P. Fulda, M.A. Arain, L. Williams, G. Mueller, D.B. Tanner, D.H. Reitze, Feedback control of optical beam spatial profiles using thermal lensing. Appl. Opt. **52**, 6452–6457 (2013)
13. *Handbook of Laser and Optics* Ed. F. Träger, (Springer Science + Business Media, LLC, New York 2007)
14. *TIE-19: Temperature Coefficient of the Refractive Index* Technical Information, Schott (2008)
15. Y. Marcus *The Properties of Solvents*, (Wiley Series in Solution Chemistry Vol. 4. Wiley, Baffins Lane 1998)
16. J.R. Whinnery, Acc. Chem. Res. **7**, 225–231 (1974)
17. L. Couston, F. Canto, Patent FR 2942873
18. J. Shen, R.D. Lowe, R.D. Snook, Chem. Phys. **165**, 385–396 (1992)
19. K. Dobek, J. Karolczak, J. Kubicki, Dyes Pigments **100**, 222–231 (2014)
20. D.R. Lide, H.V. Kehiahian, *Handbook of Thermophysical and Thermochemical Data* (CRC Press, New York, 1994)
21. K. Dobek, J. Karolczak, J. Fluorescence **22**, 1647–1657 (2012)
22. M.A. Arain, V. Quetschke, J. Gleason, L.F. Williams, M. Rakhmanov, J. Lee, R.J. Cruz, G. Mueller, D.B. Tanner, D.H. Reitze, Appl. Opt. **46**, 2153 (2007)
23. COMSOL Multiphysics 4.3 "Luneburg Lens" model example, provided with the software
24. B.E.A. Saleh, M.C. Teich, *Fundamental of Photonics* (Wiley, Singapore, 2007)
25. *Lasers and laser-related equipment—Test methods for laser beam widths, divergence angles and beam propagation ratios—Part 1: Stigmatic and simple astigmatic beams*, ISO 11146-1:2005
26. E. Krystkowiak, K. Dobek, A. Maciejewski, J. Photochem. Photobiol. A Chem. **184**, 250–264 (2006)
27. K. Dobek, J. Karolczak, D. Komar, J. Phys. Chem. A **116**, 6655–6663 (2012)
28. D.E. Wetzler, C. Chusta, R. Fernandez-Prini, P.F. Aramendia, J. Phys. Chem. A **106**, 2390–2400 (2002)
29. R. Simkovitch, S. Shomer, R. Gepshtein, D. Shabat, D. Huppert, J. Phys. Chem. A **117**, 3925–3934 (2013)
30. A. Seeboth, D. Lötzsch, *Thermochromic Phenomena in Polymers* (Smithers Rapra Technology Limited, UK, 2008)